J. Phys. G: Nucl. Phys. **8** (1982) 839–850. Printed in Great Britain

Nuclear matter distributions

J Streets, B A Brown and P E Hodgson

Nuclear Physics Laboratory, University of Oxford, Keble Road, Oxford, UK

Received 16 October 1981, in final form 23 December 1981

Abstract. The nuclear matter distributions extracted from high-energy proton scattering data for many nuclei are compared with calculations using the single-particle potential method with a standard potential.

1. Introduction

The nuclear charge distributions are now quite well known from model-independent analyses of electron elastic scattering and muonic atom data, and they can be calculated theoretically from the Hartree–Fock and single-particle potential (SPP) methods. In this context, 'model independence' means the use of a general shape for the density distribution instead of a restricted analytical expression. Nuclear matter distributions are less well known, mainly because of our lack of knowledge of the nuclear forces compared with the electromagnetic forces.

Recently, however, quite accurate nuclear matter distributions have become available, mainly from analyses of high-energy proton elastic scattering using the Glauber and Kerman–McManus–Thaler theories. By nuclear matter distribution we mean the sum of

Table 1. Parameters of the standard potential.

(*a*) Experimental data fitted.

Nucleus	E_p	E_n	r_{ch}	$r_p - r_n$	$\tilde{a}_{ch}$	$\tilde{a}_p - \tilde{a}_n$
^{40}Ca	8.33	—	3.477	—	0.521	—
^{208}Pb	8.01	7.37	5.503	−0.20†	0.512	−0.10†

† Estimates based on the result of Skyrme HF calculations and the tail densities of neutron orbits from heavy-ion sub-Coulomb stripping experiments (Durell *et al* 1976).

(*b*) Potential parameters.

Nucleus	V_p	V_n	r_p	r_n	a_p	a_n	r_C
^{40}Ca	54.08	—	1.2692	—	0.758	—	1.315
^{208}Pb	60.65	45.76	1.2675	1.238	0.810	0.716	1.198

0305-4616/82/060839 + 12$02.00

the neutron and proton distributions, whereas the charge distribution is essentially that of the protons with a small correction for the effect of the neutron charge distributions.

The SPP method has now been developed to the stage where it can reproduce the nuclear charge distributions to high accuracy (Malaguti *et al* 1978, 1979a, b, 1982, Brown *et al* 1979a, b, Hodgson 1981), and so it was considered worthwhile to collect together all the available nuclear matter distributions and to compare them with the predictions of the SPP method. This tests the usefulness of the SPP method for calculating matter distributions and also the methods used to extract them from the experimental data. The SPP method requires, for a full analysis, the data on the charge distributions, the single-particle energies and the spectroscopic factors, and for many of the nuclei studied these are not readily

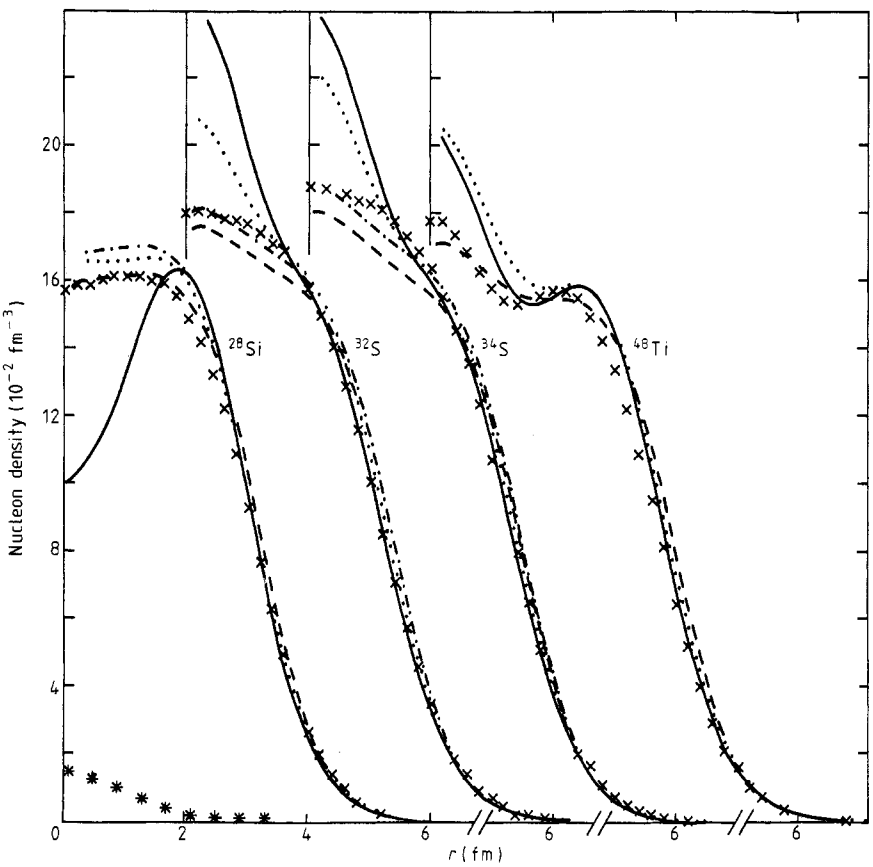

Figure 1. Nuclear matter distributions for ^{28}Si, ^{32}S, ^{34}S and ^{48}Ti compared with SPP and Hartree–Fock calculations with the standard potential. The experimental points (× × ×) are the results of a model-independent analysis of 1 GeV proton elastic scattering by Shaginyan and Starodubsky (1979). The SPP calculations were made with the occupation numbers of the simple shell model (——) and with those of Chung and Wildenthal (1978) for ^{28}Si, ^{32}S and ^{34}S, and Brown *et al* (1979a) for ^{49}Ti (· · · ·). The Hartree–Fock calculations used the same occupation numbers and the Skyrme-3 interaction (– – –). Where an appreciable difference occurs, the results of scaling the latter calculation to fit the experimental charge radius are also shown (– · – · –). The estimated uncertainty in the model-independent analysis is shown at the foot of the figures (Shaginyan and Starodubsky, private communication).

available. A preliminary analysis was therefore made using a standard potential with parameters fixed by detailed analyses of ^{40}Ca and ^{208}Pb and the results are presented here.

The form of the standard potential is described in § 2, the results of the calculations are compared with the model-independent matter distributions in § 3 and the results are discussed in § 4. All energies are in MeV and lengths in fm.

2. The standard potential

The nuclear matter distributions are calculated by summing the absolute squares of the wavefunctions of the occupied orbits, weighted by the occupation probabilities.

The potential has the form

$$V(r) = V_C(r) + Uf_1(r) + \left(\frac{\hbar}{m_\pi c}\right)^2 U_s \frac{1}{r}\frac{df_2(r)}{dr} \boldsymbol{L}\cdot\boldsymbol{\sigma} \tag{2.1}$$

where $V_C(r)$ is the electrostatic potential due to a uniformly charged sphere of radius

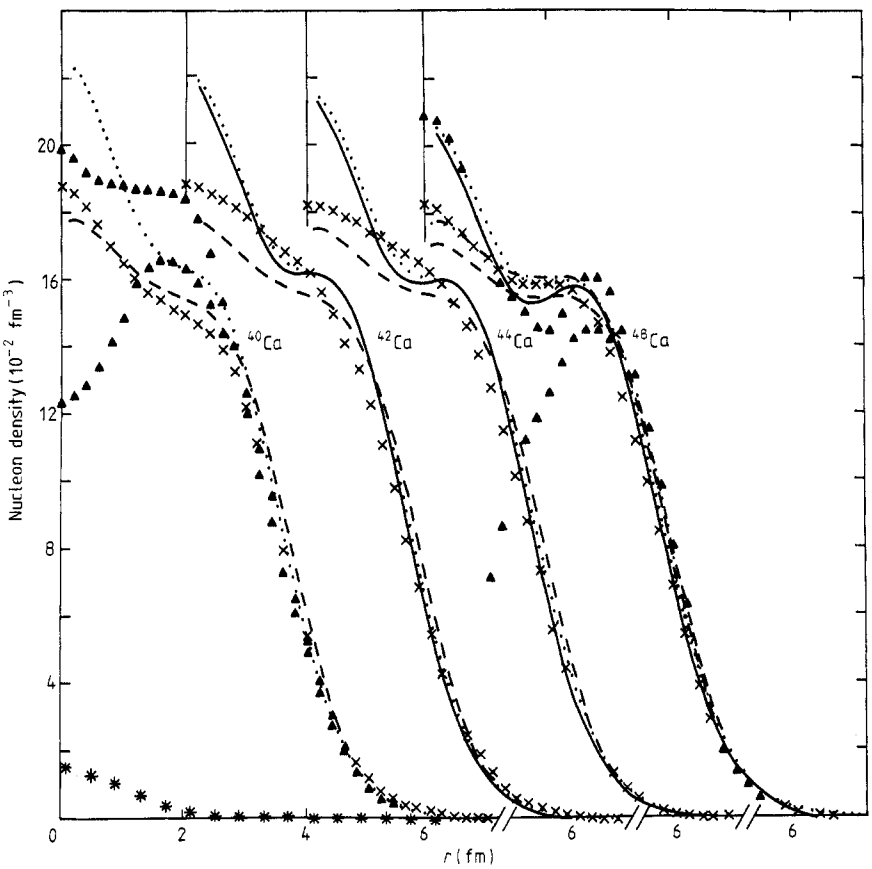

Figure 2. As figure 1 for ^{40}Ca, ^{42}Ca, ^{44}Ca and ^{48}Ca. The additional experimental points (▲▲▲) for ^{40}Ca and ^{48}Ca are the results of a model-independent analysis of 0.8 GeV proton elastic scattering by Friedman *et al* (1978). These show the upper and lower limits of the distributions obtained by the model-independent analysis.

$R_C = r_C A^{1/3}$ and charge $Z-1$, U and U_s are potential depths and the form factor $f_i(r) \equiv (1+\exp[(r-R_i)/a_i])^{-1}$ with $R_i = r_i A^{1/3}$.

The values of the parameters U, r_1 and a_1 of this potential were fixed to reproduce the experimental quantities for ^{40}Ca and ^{208}Pb listed in table 1. In this table, the diffuseness parameter $\tilde{a}$ is defined in terms of the second and fourth moments of the distribution:

$$\tilde{a} = [3(\tilde{R}_4 - \tilde{R}_2)(9\tilde{R}_2 - 7\tilde{R}_4)/2\pi^2]^{1/2} \tag{2.2}$$

where

$$\tilde{R}_L = [\tfrac{1}{3}(L+3)]^{1/L} R_L \tag{2.3}$$

and

$$R_L = \left(\frac{\int \rho(r) r^{L+2}\, d\tau}{\int \rho(r) r^2\, d\tau} \right)^{1/L}. \tag{2.4}$$

The expression (2.2) gives the surface diffuseness parameter for a Fermi distribution in the limit of large A. This serves as a convenient measure of the surface thickness. The energy E_p or E_n is that of the occupied proton or neutron state nearest the Fermi surface and the radii quoted are all point radii except for the charge distribution.

The values of the potential parameters for other nuclei were obtained using the

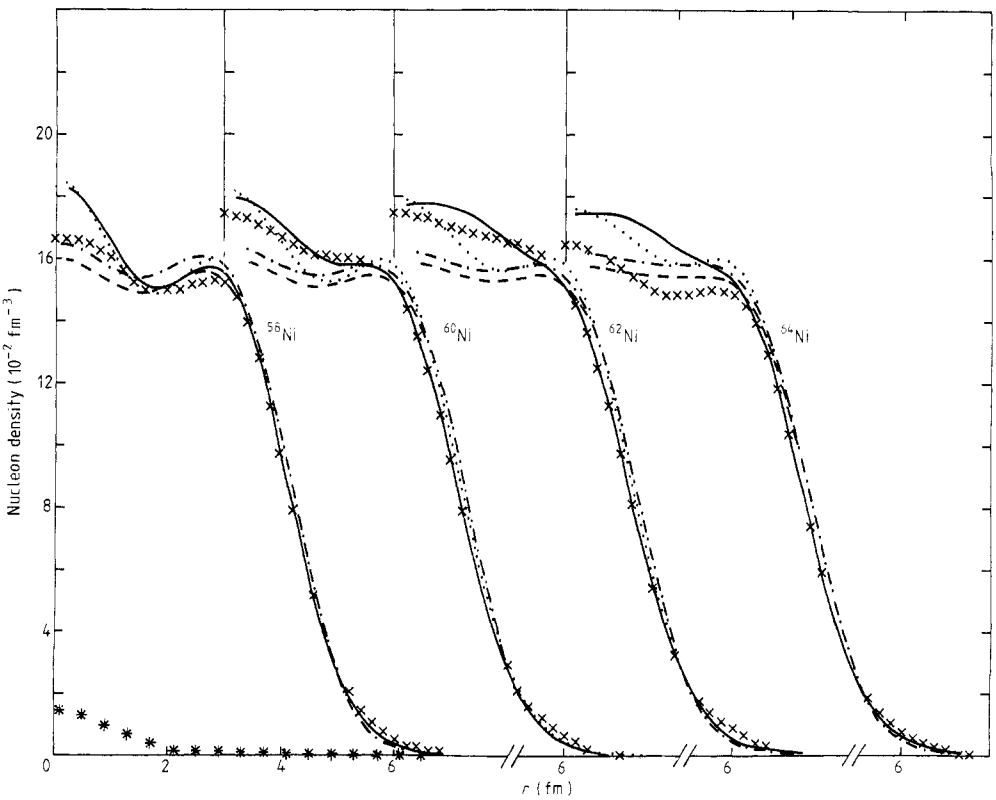

Figure 3. As figure 1 for ^{58}Ni, ^{60}Ni, ^{62}Ni and ^{64}Ni.

interpolation formula

$$X(N, Z, p/n) = X_0 \pm X_1(N-Z)/A + X_2[A^{1/3} - (208)^{1/3}] \tag{2.5}$$

where the values of X_0, X_1 and X_2 are obtained for each parameter from the three values for ^{40}Ca and ^{208}Pb in table 1; for example, the values of the potential depth are obtained from the two values of V_0 and one value of V_n. The parameters for the spin–orbit potential were fixed to the values $U_s = 6$ MeV, $r_2 = 1.1$ fm and $a_2 = 0.65$ fm. With these parameters the wavefunctions of all single-particle states, and hence the required density distributions,

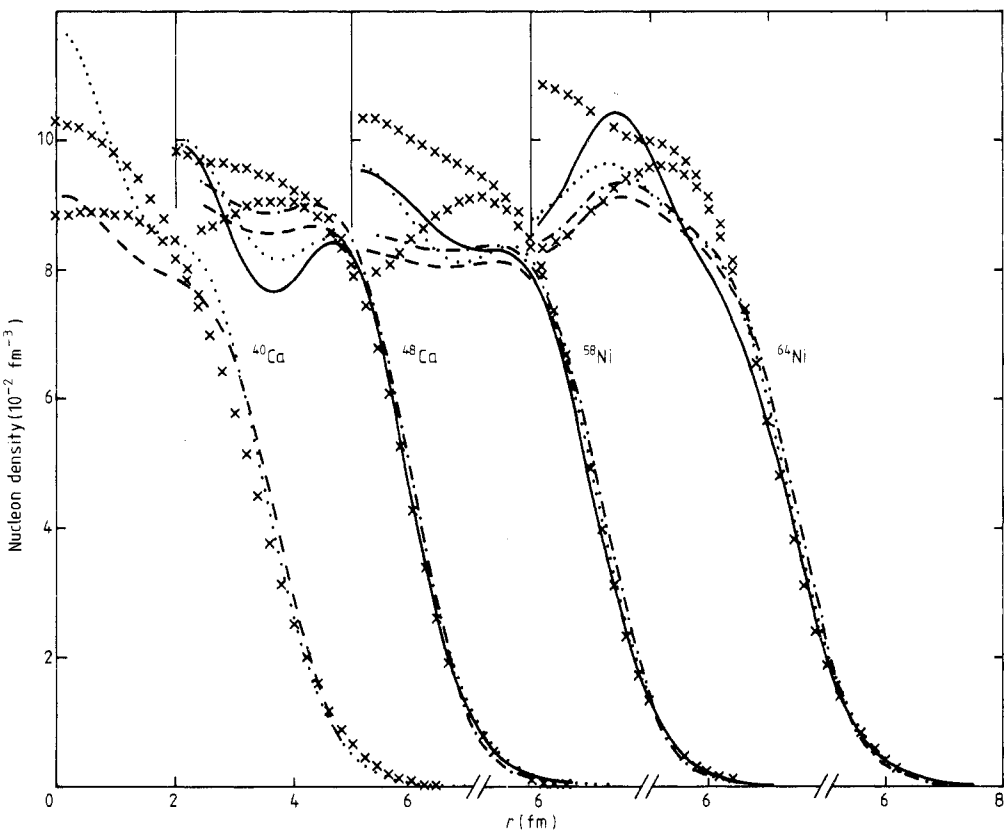

Figure 4. Neutron distributions for ^{40}Ca, ^{48}Ca, ^{58}Ni and ^{64}Ni compared with SPP and Hartree–Fock calculations with the standard potentials. The experimental points (× × ×) are the results of a model-independent analysis of 0.8 GeV proton elastic scattering by Ray (1979). These points show the upper and lower limits of the distribution obtained by the model-independent analysis. The SPP calculations were made with the occupation numbers of the simple shell model (——) and with those of Brown *et al* (1979a) for calcium and of Koops and Glaudemans (1977) for Ni (· · · ·). In the case of ^{40}Ca there is no appreciable difference between these two curves. The Hartree–Fock calculations used the same occupation numbers and the Skyrme-3 interaction (– – –). Where an appreciable difference occurs the results of scaling the latter calculation to fit the experimental charge radius are also shown (– · – · –).

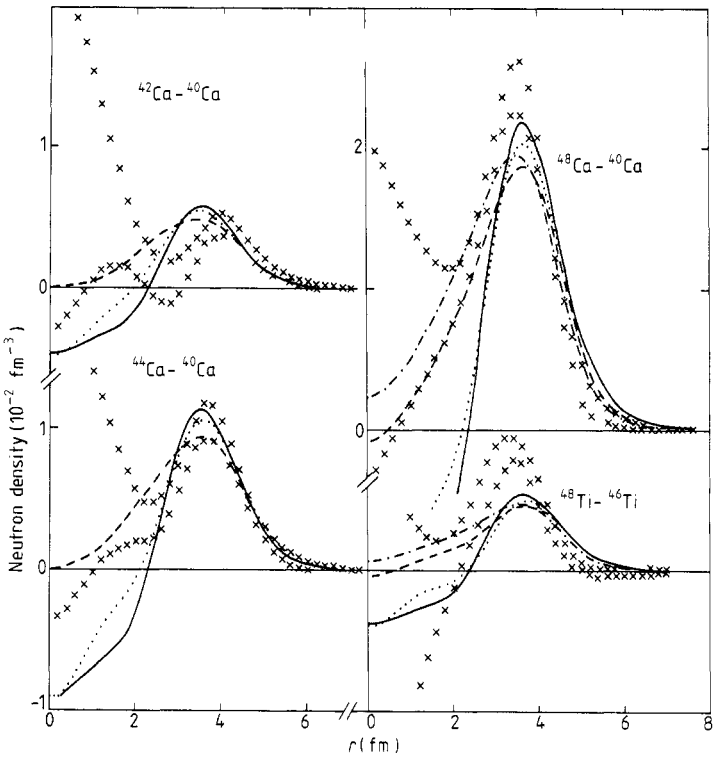

Figure 5. Neutron density differences for ^{48}Ca–^{40}Ca, ^{44}Ca–^{40}Ca, ^{42}Ca–^{40}Ca and ^{48}Ti–^{46}Ti compared with the standard potentials. The points (× × ×) show the upper and lower limits given by a model-independent analysis of 0.8 GeV proton elastic scattering by Ray *et al* (1981) in the case of calcium, and by Pauletta *et al* (1980) in the case of titanium. The SPP calculations were made with the occupation numbers of the simple shell model (——) and with those of Brown *et al* (1979a) (· · · ·). The Hartree–Fock calculations used the same occupation numbers and the Skyrme-3 interaction (– – –). Where an appreciable difference occurs the results of scaling the latter calculation to fit the experimental charge radius are also shown (– · – · –).

Table 2. Shell-model occupation numbers.

(*a*) Chung and Wildenthal (1978).

	^{28}Si		^{32}S		^{34}S	
	$\langle\pi\rangle$	$\langle\nu\rangle$	$\langle\pi\rangle$	$\langle\nu\rangle$	$\langle\pi\rangle$	$\langle\nu\rangle$
$1d_{5/2}$	4.39	4.39	5.09	5.09	5.37	5.58
$2s_{1/2}$	0.82	0.82	1.51	1.51	1.68	1.79
$1d_{3/2}$	0.79	0.79	1.41	1.41	0.95	2.63

Table 2. (continued)

(*b*) Brown *et al* (1979a).

	^{40}Ca		^{42}Ca		^{44}Ca		^{48}Ca	
	$\langle\pi\rangle$	$\langle\nu\rangle$	$\langle\pi\rangle$	$\langle\nu\rangle$	$\langle\pi\rangle$	$\langle\nu\rangle$	$\langle\pi\rangle$	$\langle\nu\rangle$
$1f_{7/2}$	0.63	0.63	1.53	1.80	1.62	3.60	0.27	7.20
$2p_{3/2}$	0.07	0.07	0.17	0.20	0.18	0.40	0.03	0.80
$1d_{3/2}$	3.30	3.30	2.30	4.0	2.20	4.00	3.70	4.00
$2s_{1/2}$	2.00	2.00	2.0	2.0	2.0	2.0	2.0	2.0
$1f_{5/2}$	0	0	0	0	0	0	0	0

(*c*) Brown *et al* (1979a).

	^{46}Ti		^{48}Ti	
	$\langle\pi\rangle$	$\langle\nu\rangle$	$\langle\pi\rangle$	$\langle\nu\rangle$
$1f_{7/2}$	3.42	3.60	2.745	5.40
$2p_{3/2}$	0.38	0.40	0.305	0.60
$1d_{3/2}$	2.20	4.00	2.95	4.00
$1f_{5/2}$	0	0	0	0

(*d*) Koops and Glaudemans (1977).

	^{58}Ni		^{60}Ni		^{62}Ni		^{64}Ni	
	$\langle\pi\rangle$	$\langle\nu\rangle$	$\langle\pi\rangle$	$\langle\nu\rangle$	$\langle\pi\rangle$	$\langle\nu\rangle$	$\langle\pi\rangle$	$\langle\nu\rangle$
$1f_{7/2}$	8.00	8.00	8.00	8.00	8.00	8.00	8.00	8.00
$2p_{3/2}$	0	1.17	0	1.98	0	2.61	—	3.15
$1f_{5/2}$	0	0.64	0	1.54	0	2.53	—	3.55
$2p_{1/2}$	0	0.19	0	0.48	0	0.86	—	1.30

(*e*) Malaguti *et al* (1979b).

	^{90}Zr	
	$\langle\pi\rangle$	$\langle\nu\rangle$
$1g_{7/2}$	0	0
$2d_{3/2}$	0	0.07
$3s_{1/2}$	0	0.04
$2d_{5/2}$	0	0.11
$1g_{4/2}$	1.45	10
$2p_{1/2}$	1.17	1.97
$2p_{3/2}$	3.61	3.94
$1f_{5/2}$	5.77	5.87
$1f_{7/2}$	8	8

(*f*) Cohen and Price (1961).

	^{116}Sn		^{124}Sn	
	$\langle\pi\rangle$	$\langle\nu\rangle$	$\langle\pi\rangle$	$\langle\nu\rangle$
$1g_{7/2}$	—	6.22	—	7.61
$2d_{5/2}$	—	4.73	—	5.58
$2d_{3/2}$	—	0.99	—	2.72
$3s_{1/2}$	—	0.83	—	1.48
$1h_{11/2}$	—	3.23	—	6.61

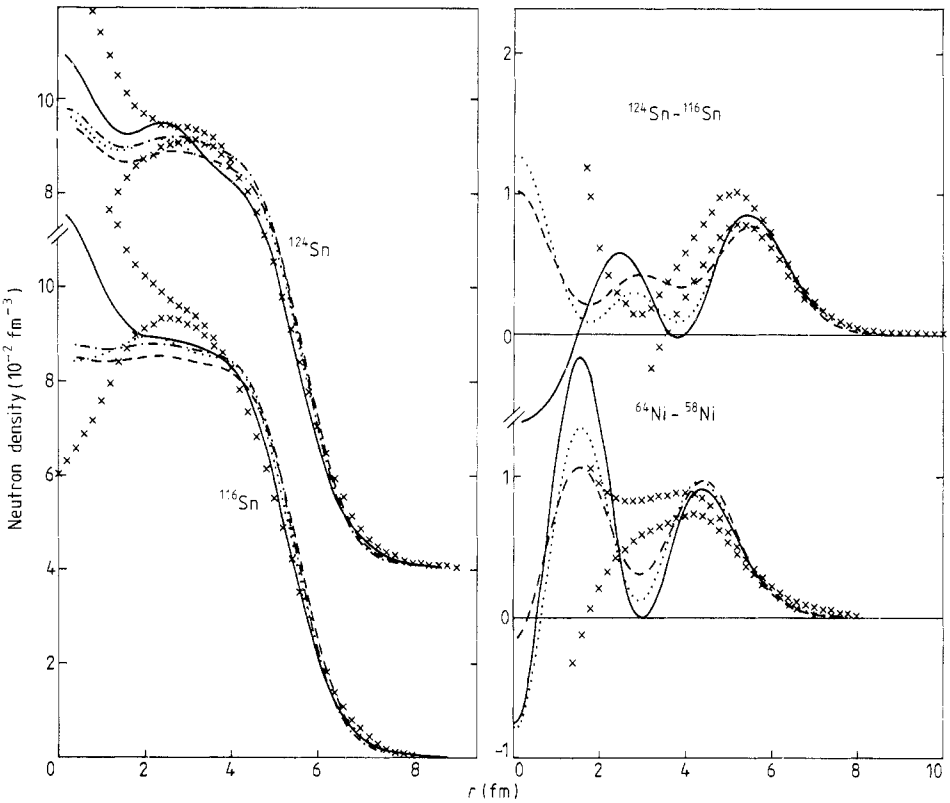

Figure 6. As figures 4 and 5 for the neutron density differences for ^{64}Ni–^{52}Ni and ^{124}Sn–^{116}Sn and neutron distributions for ^{124}Sn and ^{116}Sn (Ray and Hodgson 1979). The occupation numbers used for Ni are from Koops and Glaudemans (1977) and those for Sn are from Cohen and Price (1961).

can be calculated from the expression

$$\rho(r) = \sum_i a_i |\psi_i|^2 \tag{2.6}$$

where a_i are occupation numbers and the sum runs over all occupied orbits.

In the standard calculations the occupation numbers were set to those of the simple shell model. In some cases these were supplemented by shell-model calculations and by experimentally determined occupation numbers as described in the next section. Calculations were also made with the Hartree–Fock formalism using the Skyrme-3 interaction (Vautherin and Brink 1972, Beiner *et al* 1975). If the resulting charge distribution did not have the experimental RMS radius $\tilde{r}_{ch}$, all densities were scaled following the Tassie model using the relation

$$\tilde{\rho}(r) = \rho(r) + \tfrac{1}{2}[1 - (\tilde{r}_{ch}/r_{ch})^2][3\rho(r) + r(\mathrm{d}\rho(r)/\mathrm{d}r)] \tag{2.7}$$

which maintains the constancy of the total charge and the ratio of the mean square radii. This is the most reasonable way of adjusting the calculations to fit the known charge radii; it has a negligible effect on $r_n - r_p$.

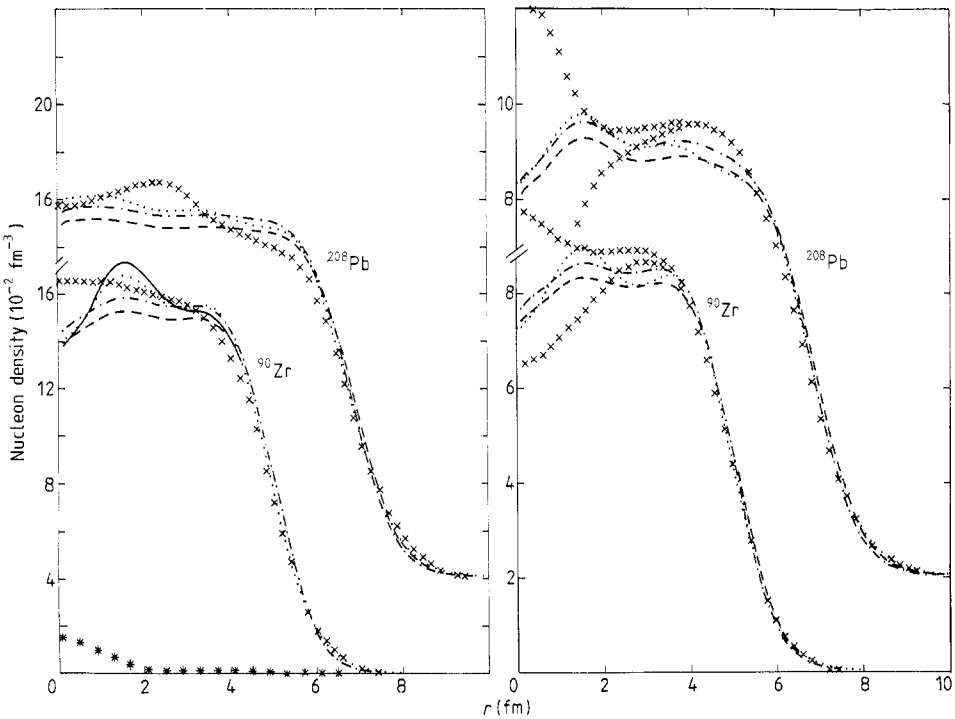

Figure 7. As figures 1 and 4 for the matter and neutron distributions of ^{90}Zr and ^{208}Pb. For ^{208}Pb simple shell-model occupation numbers are used throughout. The experimental points ($\times$ $\times$ $\times$) for the neutron distributions are the results of a model-independent analysis of 0.8 GeV proton elastic scattering by Hoffmann *et al* (1980) for ^{208}Pb and by Ray *et al* (1978a) for ^{90}Zr. The estimated uncertainty in the model-independent analysis of the nuclear matter distributions is shown at the foot of the figure.

3. Comparison between measured and calculated matter distributions

The nuclear matter distributions for several nuclei were calculated using the method described in § 2, and the results are compared in figures 1–7 with those obtained from analyses of experimental data. Also included are the corresponding comparisons for neutron density differences between adjoining nuclei.

On the whole the agreement is good, particularly in the surface region which is the most important for reaction calculations. For closed-shell nuclei it is expected that the occupation numbers are those of the simple shell model. In other cases this is less accurate and so calculations are also made using occupation numbers obtained from shell-model calculations and from experimental data on nucleon transfer reactions. These are listed in table 2.

In a few cases (^{40}Ca, ^{48}Ca) two results of analyses of experimental data are available and they are not consistent with each other. The calculations are more in accord with the later data of Shaginyan and Starodubsky (1979) in both cases.

A further comparison with experiment is provided by the RMS charge radii, and with the differences between the neutron and proton RMS radii, where available. These are listed in tables 3 and 4 and again show overall agreement.

Table 3. Charge radii (fm).

Nucleus	Experimental	Calculated		
		A	B	C
^{28}Si	3.125(3)[a]	3.205	3.234	3.181
^{32}S	3.263(2)[a]	3.323	3.329	3.297
^{34}S	3.264[a,b]	3.312	3.313	3.309
^{40}Ca	3.483(3)[c]	3.477	3.499	3.487
^{42}Ca	3.513(3)[c]	3.464	3.518	3.513
^{44}Ca	3.524(3)[c]	3.456	3.512	3.525
^{48}Ca	3.482(3)[c]	3.452	3.463	3.528
^{46}Ti	3.614(4)[c]	3.576	3.631	3.611
^{48}Ti	3.599(4)[c]	3.570	3.603	3.610
^{58}Ni	3.777(5)[d]	3.845	3.846	3.819
^{60}Ni	3.815(6)[d]	3.846	3.850	3.845
^{62}Ni	3.844(5)[d]	3.852	3.855	3.871
^{64}Ni	3.862(5)[d]	3.861	3.863	3.896
^{90}Zr	4.2633(84)[e]	4.251	4.270	4.316
^{116}Sn	4.619(4)[f]	4.620	4.617	4.669
^{124}Sn	4.670(5)[f]	4.654	4.651	4.727
^{208}Pb	5.503[g]	5.503	5.503†	5.569†

A, Saxon–Woods; B, Saxon–Woods and various occupation numbers; C, Skyrme-3 and various occupation numbers.
[a]Schaller *et al* (1978); [b]Brown *et al* (1980); [c]Wohlfahrt *et al* (1981); [d]Wohlfahrt *et al* (1980); [e]Rothhaas (1976); [f]Ficenec *et al* (1972); [g]Frois *et al* (1977), Friar and Negele (1973).
† No variation in occupation numbers, closed shells assumed.

Table 4. Proton–neutron radius difference (fm).

Nucleus	Experimental	Calculated		
		A	B	C
^{28}Si	0.01(10)[e]	0.065	0.074	0.040
^{32}Si	0.00(10)[e]	0.078	0.080	0.043
^{34}S	—	−0.029	−0.028	−0.026
^{40}Ca	0.0(1)[c,d]	0.089	0.090	0.045
^{42}Ca	−0.00(4)[f]	−0.030	0.014	−0.002
^{44}Ca	−0.02(4)[f]	−0.128	−0.089	−0.054
^{48}Ca	−0.11(4)[f]	−0.284	−0.292	−0.152
^{46}Ti	0.08(7)[b]	−0.005	0.037	0.014
^{48}Ti	−0.06(7)[b]	−0.090	−0.071	−0.040
^{58}Ni	−0.01(5)[d]	0.030	0.030	0.006
^{60}Ni	—	−0.039	−0.038	−0.033
^{62}Ni	—	−0.107	−0.097	−0.067
^{64}Ni	−0.18(5)[d]	−0.156	−0.150	−0.098
^{90}Zr	−0.085(50)[d]	−0.109	−0.097	−0.053
^{116}Sn	−0.13(5)[d]	−0.111	−0.128	−0.081
^{124}Sn	−0.22(5)[d]	−0.232	−0.241	−0.137
^{208}Pb	−0.14(4)[a]	−0.198	−0.126†	−0.126†

A, Saxon–Woods; B, Saxon–Woods and various occupation numbers; C, Skyrme-3 and various occupation numbers.
[a]Hoffmann *et al* (1980); [b]Pauletta *et al* (1980); [c]Brown *et al* (1979a); [d]Ray (1980); [e]Alkhazov *et al* (1978); [f]Brown *et al* (1979b).
† Closed shells assumed.

The results for the neutron distribution differences in figures 5–7 show considerable divergences, particularly in the nuclear interior. The results for the nuclei ^{44}Ca–^{40}Ca and ^{48}Ca–^{40}Ca in figure 5 are appreciably better than those for other nuclei. It is likely that the deficiencies in the interior are to some extent attributable to the use of a Saxon–Woods potential; recent studies on ^{208}Pb show that the interior charge density can only be reproduced by a potential with some oscillatory behaviour in the interior (Brown 1981, private communication) and similar effects may be present in lighter nuclei.

It is concluded that the single-particle potential model with the standard potential provides a satisfactory way of calculating the overall features of nuclear matter distributions but that further work is necessary to understand some of the detailed discrepancies that remain. In particular, further work is needed on the methods used to extract the matter distributions from the experimental data in order to improve their accuracy and also to remove existing discrepancies. This will provide stimulus for more precise theoretical analyses.

References

Alkhazov G D, Belostotsky S L and Vorobyov A A 1978 *Phys. Rep.* **42** 89

Beiner M, Flocard H, Van Giai N and Quentin P 1975 *Nucl. Phys.* A **238** 29

Brissaud I and Campi X 1978 *Vancouver Conf. on High Energy Physics and Nuclear Structure* Abstract

Brown B A, Chung W and Wildenthal B H 1980 *Phys. Rev.* C **22** 774

Brown B A, Massen S E and Hodgson P E 1979a *J. Phys. G: Nucl. Phys.* **5** 1655

—— 1979b *Proc. Int. Meeting on the Radial Shape of Nuclei in the Calcium Region, Karlsruhe* p 377

Chung W and Wildenthal B H 1978 to be published

Cohen B L and Price R E 1961 *Phys. Rev.* **121** 1441

Durell J L, Buttle P J A, Goldfarb L J B, Phillips W R, Jones G D, Hooton B W and Ivanovich M 1976 *Nucl. Phys.* A **269** 443

Ficenec J R, Fajardo L A, Trower W P and Sick I 1972 *Phys. Lett.* **42B** 213

Friar J L and Negele J W 1973 *Nucl. Phys.* A **212** 93

Friedman E, Gils H J, Rebel H and Majka Z 1978 *Phys. Rev. Lett.* **41** 1220

Frois B, Bellicard J B, Cavedon J M, Huet M, Leconte P, Ludeau P, Nakada A, Hô Phan Zuan and Sick I 1977 *Phys. Rev. Lett.* **38** 152

Hodgson P E 1981 *Notas de Fisica* **4** 169

Hoffmann G W, Ray L, Barlett M, McGill J, Adams G S, Igo G J, Irom F, Wang A T M, Whitten C A Jr, Boudre R L, Amann J F, Glashausser C, Hintz N M, Kyle G S and Blanpied G S 1980 *Phys. Rev.* C **21** 1488

Koops J E and Glaudemans P W M 1977 *Z. Phys.* A **280** 181

Malaguti F, Uguzzoni A, Verondini E and Hodgson P E 1978 *Nucl. Phys.* A **297** 287

—— 1979a *Nuovo Cimento* A **49** 412

—— 1979b *Nuovo Cimento* A **53** 1

—— 1982 *Riv. Nuovo Cimento* in press

Pauletta G, Adams G, Gazzaly M M, Igo G J, Wang A T M, Rahbar A, Wriekat A, Ray L, Hoffmann G W, Barlett M and Amann J 1980 *Proc. Int. Conf. on Nuclear Physics, Berkeley* Abstracts p 115

Platchkov S K, Bellicard J B, Cavedon J M, Frois B, Goutte D, Huet M, Leconte P, Hô Phan Zuan, de Witt Huberts P K A, Lapikás R and Sick I *Preprint*

Ray L 1979 *Phys. Rev.* C **19** 1855

—— 1980 *Nucl. Phys.* A **335** 443

Ray L, Coker W R and Hoffmann G W 1978a *Phys. Rev.* C **18** 2641

Ray L and Hodgson P E 1979 *Phys. Rev.* C **20** 2403

Ray L, Hoffmann G W, Barlett M, McGill J, Amann J, Adams G, Pauletta G, Gazzaly M and Blanpied G S 1981 *Phys. Rev.* C **23** 828

Ray L, Hoffmann G W, Blanpied G S, Coker W R and Liljestrand R P 1978b *Phys. Rev.* C **18** 1756

Rothhaas H 1976 *Dissertation* Universität Mainz

Schaller L A, Dubler T, Kaeser K, Rinker G A, Robert-Tissot B, Schellenberg L and Schneuwly H 1978 *Nucl. Phys.* A **300** 225
Shaginyan V R and Starodubsky V E 1979 *Leningrad Nuclear Physics Institute Preprint No 457*
Starodubsky V E and Shaginyan V R 1978 *Leningrad Nuclear Physics Institute Preprint No 387*
Vautherin D and Brink D M 1972 *Phys. Rev.* C **5** 626
Wohlfahrt H D, Schwentker O, Fricke G, Andresen H G and Shera E B 1980 *Phys. Rev.* C **22** 264
Wohlfahrt H D, Shera E B, Hoehn M V, Yamazaki Y and Steffen R M 1981 *Phys. Rev.* C **23** 533